

Simulating Deflagrations and Detonations with Detailed Chemistry

Florian Ettner, Klaus G. Vollmer, Thomas Sattelmayer

Lehrstuhl für Thermodynamik, Technische Universität München
85747 Garching, Germany

1 Introduction

When simulating detonations or the transition from a deflagration to a detonation (DDT), recent publications are often focused on high spatial resolution while chemistry is reduced to a one-step or two-step mechanism. This leads to good results when simulating established detonations, but in the case of DDT reaction parameters usually require a fit to the specific problem. Moreover, experiments have shown that quenching and reignition can play an important role for the onset of DDT. For this reason a reliable numerical tool for the investigation of DDT should include a chemical mechanism as accurate as possible.

2 Combustion Model

When simulating a reactive flow there exist a variety of techniques to reduce the complexity of the chemical mechanism. Most of these techniques require extensive preprocessing of the mechanism and the resulting simplified mechanism is often limited to a narrow range of physical parameters. This is a big problem when simulating instationary problems including flame acceleration where physical parameters vary considerably during the run. For the computations presented here we did not reduce the mechanism prior to the computation. Instead, we took the full Jachimowski reaction mechanism [1] (9 species, 20 reactions, N_2 inert) which had initially been developed for hydrogen combustion at moderate pressures but has been applied successfully to reactive flows at elevated pressures, too.

We solve the reactive Reynolds-averaged Navier-Stokes equations including 8 transport equations for the reactive species O_2 , H_2 , H_2O , O , H , OH , HO_2 and H_2O_2 . The source terms of these equations are calculated by integrating the Arrhenius-type elementary reactions of the Jachimowski mechanism with a fourth-order Rosenbrock method. Each result of such an integration step is saved in a dynamic 10-dimensional reaction map having temperature and the 9 species concentrations as coordinates. Whenever a new source term is required the solver checks whether a source term in the near proximity (“basepoint” BP) of the current state has already been calculated. In that case, the source term $\vec{\omega}$ for each species between the time steps n and $n + 1$ can be gained via a linear interpolation

$$\vec{y}_{n+1} = \vec{y}_n + (\vec{y}_{n+1} - \vec{y}_n)_{BP} + \left(\frac{\partial \vec{y}_{n+1}}{\partial \vec{y}_n} \right)_{BP} (\vec{y}_n - \vec{y}_{n,BP}) \quad (1)$$

$$\vec{\omega} = \frac{\vec{y}_{n+1} - \vec{y}_n}{t_{n+1} - t_n} \quad (2)$$

where \vec{y}_n denotes the state vector of the variables temperature and species concentrations at time step n and t_n denotes the respective time.

Only if no basepoint for the current state is found, the mechanism is solved directly and the result \vec{y}_{n+1} at this new basepoint is stored in the reaction map together with its Jacobian matrix $(\partial\vec{y}_{n+1}/\partial\vec{y}_n)_{\text{BP}}$. The computation of the Jacobian might seem costly at first but it soon pays off because the number of new basepoints to be calculated rapidly decreases during the run so that the majority of source terms can be accessed from the reaction map [2]. Fig.1 illustrates that the resulting reaction map of basepoints is sparsely populated which makes the combustion model much more efficient than a preprocessing technique where a complete state space has to be evaluated before starting the computation of the flow.

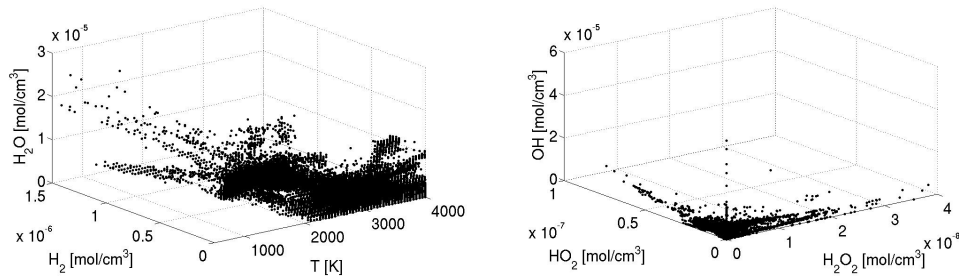


Figure 1: Visualization of the reaction map in three dimensions. Left: $T-H_2-H_2O$ space. Right: $H_2O_2-HO_2-OH$ space. Black dots indicate points where the reaction has been evaluated.

3 Application to flame acceleration and detonation

In order to demonstrate the capability of this model the combustion of a hydrogen-air mixture in a closed channel with periodic obstacles is simulated. The geometry consists of a 5700 mm long channel with a height of 60 mm. Periodic obstacles with a blockage ratio $BR = 60\%$ are placed at a distance of 100 mm. The last obstacle is at a distance of 3000 mm from the left end, the remainder of the channel is smooth. The fluid is at rest at the start of the simulation. Ignition is achieved by patching a small region next to the left end of the channel to an elevated temperature. The simulation is run on a rather coarse, two-dimensional mesh (2.5 mm x 2 mm rectangular cells). Turbulence is modelled with the standard $k-\varepsilon$ -model. A free slip boundary condition is placed on the adiabatic walls. The discretisation is second order both in space and time.

In the following we present the results for two different cases: one with a stoichiometric hydrogen-air mixture (case A) and one with a lean mixture (case B, hydrogen mole fraction $x_{H_2} = 13\%$). The mixture composition of case B has been chosen because different researchers [3, 4] reported the occurrence of DDT in channels of various sizes for hydrogen mole fractions a little above this value.

In Fig. 2 the flame position over time is plotted for both cases. It was defined by determining the rightmost point on the center line of the channel where water is formed ($\dot{\omega}_{H_2O} > 0$). It can be seen that in both cases the flame propagation starts as a slow deflagration. However, the flame in the stoichiometric mixture quickly accelerates up to a constant velocity of 1720 m/s, corresponding to approximately 88 % of the Chapman-Jouguet (CJ) velocity u_{CJ} of the mixture. Only after leaving the obstacle region ($x > 3000$ mm) it accelerates once more to a final velocity of 2020 m/s. In the lean mixture, the flame accelerates more gradually to a final velocity of 605 m/s. This corresponds to approximately 43 % of the CJ velocity of the mixture.

Although the propagation speed of both flames is quite different, a leading shock in front of the flame is observed in both cases. Based on a common rule of thumb (see e.g. [3]), flame propagation velocities $u > 0.5 u_{CJ}$ are typical for detonations while propagation velocities between this value and the speed of sound, $c < u < 0.5 u_{CJ}$, indicate fast deflagrations.

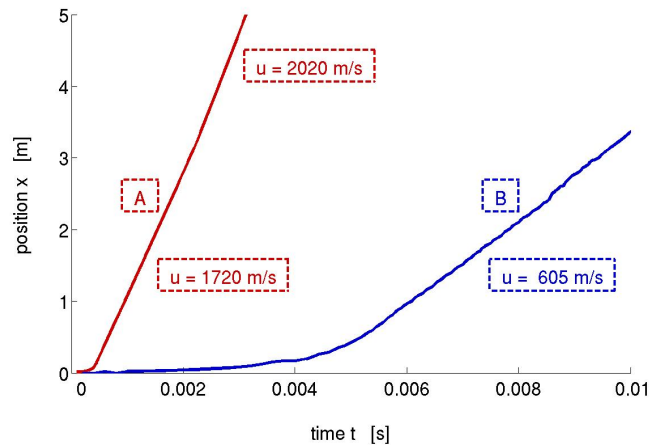


Figure 2: Flame position over time.

The results of case A can be identified as a detonation. From the pressure and temperature distribution in Fig. 3 it can clearly be seen that the flame immediately follows the shock. The leading shock (Mach number $M = 4.2$) compresses the unburnt mixture to a pressure of 20 bar and a temperature of 1280 K. Employing the Jachimowski mechanism, the ignition delay time at this state can be determined to $t_{\text{ig}} = 2 \cdot 10^{-5}$ s. Combining this value with the local velocity of the flow after the shock, a theoretical distance between shock and flame of 5.5 mm is obtained. However, as the numerical discretisation scheme needs more than one cell to resolve the shock, the flame in Fig. 3 follows the shock quasi immediately.

The continuous shock reflections at the obstacles can be seen as inhibitors for reaching the theoretical Chapman-Jouguet velocity of an unconfined mixture. After each obstacle the part of the detonation front which passed through the middle of the channel expands again in the transverse direction which leads to a curved detonation front. Consequently not the complete energy of reaction feeds into the momentum in the axial direction. Having passed the final obstacle at $x = 3000$ mm, the curved shock front becomes plane and the detonation accelerates to a velocity of 2020 m/s, approximately 103 % of the Chapman-Jouguet velocity of the mixture.

While the reaction in a detonation is achieved purely by the temperature rise caused by the leading shock, the temperature rise due to the leading shock in a fast deflagration is not sufficient for self-ignition. Consequently the flame in a fast deflagration is decoupled from the shock and its structure can be highly wrinkled. This experimental observation [3] was reproduced in the simulation of case B. In Fig. 3 temperature and pressure of the flow field shortly after passing the final obstacle are displayed on the right. The after-shock temperature is by far too low to initiate self-ignition of the combustible mixture. Nevertheless the flame follows the shock at a nearly constant distance of 10 cm. However its shape is not as plane as the shock but asymmetric and highly wrinkled, even on the macroscopic scale. This is a clear sign that the combustion is not initiated by the shock. The shock simply causes the unburnt fluid to accelerate and carry the flame away with itself. In the gap between shock and flame there is an average flow velocity of 485 m/s, thus the net velocity of the flame relative to its surrounding is just a little above 100 m/s which is far below the local speed of sound. It can be concluded that although the reaction propagates at supersonic speed inside the channel, its propagation mechanism is not a detonation but a fast deflagration.

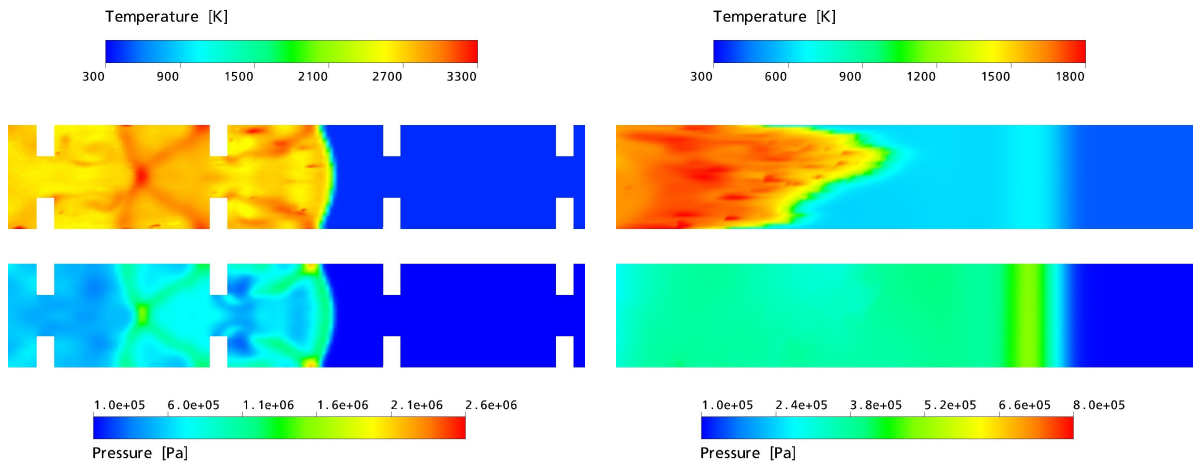


Figure 3: Temperature and pressure distribution. Left: detonation within the obstacle region (case A). Right: fast deflagration shortly after passing the final obstacle (case B).

4 Conclusions and Outlook

The construction of a combustion model using full transport equations for all reactive species is demonstrated. The computational effort solving chemical reaction is minimized by an on-the-fly reaction mapping mechanism. It has been shown that this model is capable of qualitatively simulating both deflagrations and detonations and especially the transition between both regimes.

In order to improve the simulated flame velocities in the deflagration regime, a suitable model for turbulence-chemistry interaction will be included in the model. In the future, simulations in partially open tubes and in non-homogeneous mixtures will be carried out. In combination with experimental investigations, reliable criteria for the onset of DDT are to be deduced.

Acknowledgements

This project is funded by the German Federal Ministry of Economics and Technology based on a ruling of the German Bundestag (*Förderkennzeichen 1501338*) which is gratefully acknowledged. The responsibility for the content is with the authors.

References

- [1] Jachimowski CJ. (1988). An analytical study of the hydrogen-air reaction mechanism with application to scramjet combustion. NASA TP 2791
- [2] Förster H, Sattelmayer T. (2006). Computationally Efficient Tabulation of H₂-Air Combustion with Turbulence-Chemistry Interaction. 14th AIAA/AHI Int. Space Planes and Hypersonic Sys. and Techn. Conf.
- [3] Eder A, Gerlach C, Mayinger F. (2000). Experimental observation of fast deflagrations and transition to detonations in hydrogen-air-mixtures. Proc. Symp. Energy Engineering in the 21st Century
- [4] Dorofeev SB et al. (1996). Deflagration to detonation transition in large confined volume of lean hydrogen-air mixtures. Combust. Flame 104: 95